AJNR Am J Neuroradiol 23:1206–1213, August 2002

Anatomic Features Predictive of Complete Aneurysm Occlusion Can Be Determined with Three-Dimensional Digital Subtraction Angiography

Hiro Kiyosue, Shuichi Tanoue, Mika Okahara, Yuzo Hori, Takaharu Nakamura, Hirofumi Nagatomi, and Hiromu Mori

BACKGROUND AND PURPOSE: **Complete occlusion of intracranial aneurysms is the goal of endovascular treatment and is influenced by several aneurysm-related anatomic factors. The anatomic features of aneurysms can be characterized by three-dimensional reconstructed images by use of rotational digital subtraction angiography (3D-DSA). The purpose of this study was to determine the anatomic factors that could help predict complete endosaccular packing of cerebral aneurysms by use of 3D-DSA and to design a simple scoring system to predict the difficulty of achieving complete occlusion of the aneurysm.**

METHODS: **Forty-seven patients with 47 intracranial berry (<12 mm) aneurysms underwent 3D-DSA. Aneurysms were subsequently treated by endosaccular packing with coils. The following aneurysm-related anatomic parameters were measured on 3D-DSA images: largest diameter, neck size, dome-to-neck ratio, shape, and relationship to the neighboring artery. The relationship between each parameter and the rate of successful treatment was determined, and a score used to rate difficulty of attaining occlusion (ie, difficulty score) was developed on the basis of the identified predictors of successful treatment. Subsequently, we assessed the correlation between the score and the rate of successful occlusion.**

RESULTS: **Four anatomic parameters correlated significantly with the rate of successful occlusion: neck size ($P = .014$), shape ($P = .042$), dome-to-neck ratio ($P < .01$), and relationship to neighboring artery ($P = .025$). The difficulty score based on two parameters (dome-to-neck ratio and relationship to neighboring artery) significantly correlated with the occlusion rate ($r = 0.63$, $P < .01$).**

CONCLUSION: **In this population, the difficulty score based on 3D-DSA findings provides useful information for prediction of successful endovascular treatment for intracranial aneurysms.**

Endosaccular packing of cerebral aneurysms by Guglielmi detachable coils (GDCs) has been widely used since their introduction in 1991 (1–3). Complete occlusion of the intracranial aneurysm without any complications is the goal of endovascular treatment with GDC. The treatment outcome may be influenced by several factors, including aneurysmal morphology (dome-to-neck ratio, size of the neck and dome, shape), location, relationship to the major neighboring artery, tortuousity of the parent artery, and experience of the operator. It has been reported that the most important predictive factors of successful treatment are aneurysmal neck size, dome-to-neck ratio, and size of the aneurysm (4–6). The relationship of the aneurysm to the neighboring artery is also an important factor in determining the feasibility of the GDC procedure. However, these morphologic and anatomic factors cannot be accurately determined by conventional biplane digital subtraction angiography (DSA). Recent developments in technology have enabled us to obtain three-dimensional reconstructed images by use of rotational digital subtraction angiography (3D-DSA) (7–11). To date, 3D-DSA may produce the clearest three-dimensional im-

Received December 3, 2001; accepted after revision March 17, 2002.

From the Department of Radiology (H.K., S.T., H.M.), Oita Medical University, and the Departments of Radiology (M.O., Y.H.) and Neurosurgery (T.N., H.N.), Nagatomi Neurosurgical Hospital, Oita, Japan.

Address reprint requests to Hiro Kiyosue, MD, Department of Radiology, Oita Medical University, I-i, Hasama-machi, Oita 870-0822, Japan.

ages and is useful for clinical decision making regarding endovascular treatment of the aneurysm (8, 10–12).

In the present study, we measured several aneurysm-related morphologic factors, including largest diameter of the sac, size of the neck, dome-to-neck ratio, shape, and relationship to the neighboring artery by using 3D-DSA. We then devised a simple scoring system based on these factors to predict difficulty of complete occlusion with GDC and assessed the correlation between the score and the occlusion rate of the aneurysm.

Methods

Patients

From March 1999 until October 2001, coil embolization was scheduled for 52 intracranial aneurysms in 52 patients. All patients were selected for coil embolization after evaluation of cerebral arteriographic results, including 3D-DSA and clinical data by neuroradiologists (H.K., S.T.) and neurosurgeons (T.N., H.N.). Selection for coil embolization was restricted to poor surgical conditions based on the presenting medical conditions (high Hunt and Kosnik grades, associated general complications such as ischemic heart disease or cerebral ischemic diseases, or age >75 years) and location of the aneurysm (difficult surgical access).

Two cases with fusiform aneurysms were treated by parent artery occlusion by using coils. In three cases, the GDC procedure was interrupted before the detachment of the first coil because of poor maneuverability of the microcatheter caused by significant tortuousity of the access root. These five cases were excluded from this study. The remaining 47 cases were treated by endosaccular packing with GDCs. They included 13 men and 34 women with ages ranging from 31 to 88 years (mean age, 65 years). Thirty-three of the 47 patients had subarachnoid hemorrhage revealed by CT at admission. The aneurysms were located in the internal carotid artery (n = 21), anterior communicating artery (n = 9), basilar artery (n = 8), middle cerebral artery (n = 2), posterior communicating artery (n = 2), posterior cerebral artery (n = 2), anterior cerebral artery (n = 2), and vertebral artery (n = 1).

Angiography

All procedures were performed using a biplane DSA unit (Advantx LCN Plus, GE Medical Systems, Milwaukee, WI). A workstation (Advantage Workstation 3.1, GE Medical Systems) with data from rotational angiographies was used to perform 3D-DSA. Rotational angiography was performed with a 200° rotation of the C-arm in 5 seconds. Radiographic exposures were made at a frame rate of 8.8/s during the rotational procedure. The matrix size of each frame was 512 × 512 pixels. For each patient, 15 to 25 mL of contrast medium (iohexol, 300 mg/dL) was injected at a rate of 3 to 5 mL/s with a catheter positioned at the cervical portion of the carotid artery or vertebral artery. Both mask data and contrast data were electronically transferred to the workstation. A three-dimensional reconstruction algorithm based on an algebraic reconstruction technique was used to digitally produce 3D-DSA images on the workstation within 8 minutes. Reconstructed images, including maximum intensity projection (MIP), surface shaded display, and virtual endoscopic view, were made available from the data. Minimum density threshold processing was usually automatically performed at the same value (1100). In cases requiring evaluation of the relationship between the aneurysm and small neighboring artery, the processing was performed manually by two neuroradiologists (H.K., S.T.) using conventional DSA images as a reference. An artifact of surface shaded display caused by partial volume averaging at the neck of the aneurysm is well known (11). Therefore, we used MIP images for calculation of the neck of the aneurysm, except for cases in which MIP images provided insufficient definition of the neck.

Embolization

In 33 of 47 aneurysms, endovascular treatment was performed during the same angiographic session. All procedures except one were performed with the patient under general anesthesia. Systemic heparinization was performed during the procedure, which commenced after placement of the first coil into the aneurysmal sac in treatment of the ruptured aneurysm. The appropriate size of the GDC for each aneurysm was determined by measurement of the short axial diameter of the dome by using the workstation. GDCs were placed in the desired location under biplane fluoroscopic guidance with road mapping. The biplane C-arm was positioned at the appropriate projection after determination of the best angle to show the aneurysmal neck by using 3D-DSA images. Complex techniques, such as the remodeling technique with balloon (13) and the double microcatheter technique (14), were used in 10 procedures. Biplane DSA images and 3D-DSA images were obtained again immediately after the procedure.

Analysis of Aneurysms

Two neuroradiologists (S.T., M.O.) independently retrospectively assessed the 3D-DSA images. Differences in assessment of both observers were resolved by consensus. The following features of the aneurysms were assessed: largest diameter of the sac, size of the neck, shape, dome-to-neck ratio, and relationship to the neighboring artery.

Largest Diameter.—The largest diameter of the aneurysmal sac was calculated on the workstation by using MIP images. The aneurysms were divided into two groups according to the largest diameter, using a cutoff value of 5 mm: the classification of small indicated aneurysms less than 5 mm in diameter and medium indicated diameter of 5 mm or larger. None of the aneurysms in this series had a diameter greater than 12 mm.

Neck Size.—Neck size represented the largest axial diameter at the orifice of the aneurysms calculated on the workstation. The aneurysms were divided into two groups according to neck size, using a cutoff value of 4 mm: small size indicated a neck size of less than 4 mm; wide size, necks equal to or larger than 4 mm.

Shape.—Aneurysms were classified into those with simple shapes and those with complex shapes. Simple shapes included round and oval shapes, with or without small blebs. Complex shapes included multilobulated and mushroom shapes.

Dome-to-Neck Ratio.—The dome size used for the dome-to-neck ratio was the smallest axial diameter of the dome. For aneurysms with complex shapes, the smallest axial diameter of the proximal dome was used as the dome size (Fig 1). Aneurysms were divided into three groups according to dome-to-neck ratio: those less than 1.2, those between 1.2 to 1.5, and those greater than 1.5.

Relationship to Major Neighboring Artery.—This feature determined whether the aneurysm had a branch vessel arising from the aneurysmal neck and was classified as separate or involved.

Occlusion Rate Immediately after Embolization.—The level of aneurysmal occlusion after embolization was classified on the basis of both 2D-DSA and 3D-DSA findings by using the classification system presented by Cognard et al (15): 100% occlusion, sac and neck are densely packed; greater than or equal to 95% occlusion, sac is occluded but an obvious small remnant neck or suspicion of a remnant neck exists; less than

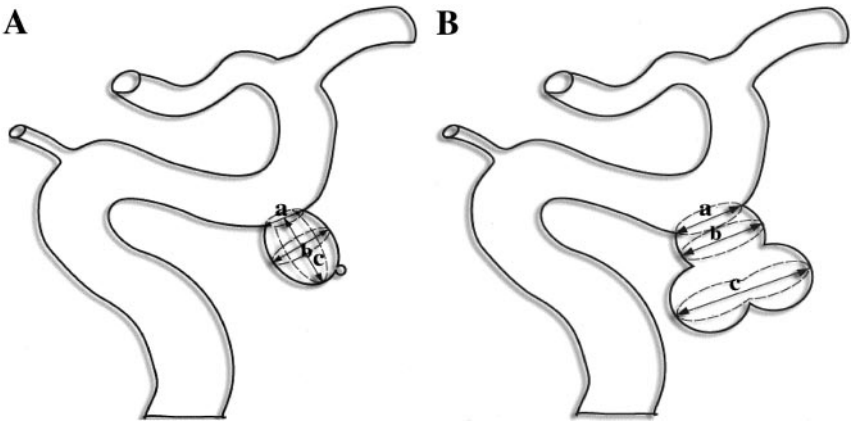

FIG 1. Schematic drawings show measurement of aneurysmal diameters in aneurysms with simple and complex shapes.

A, An aneurysm with simple shape (oval with a small bleb). Neck size (*a*) used in this study is the largest axial diameter of the orifice of the aneurysm. Dome size used for the dome-to-neck ratio is a short axial diameter of the dome (*b*). Estimation of the maximum diameter of the sac is shown (*c*). The small bleb is not included when estimating the maximal diameter of the sac.

B, Aneurysm with complex shape (multilobular). Dome size used for the dome-to-neck ratio in this type is the short axial diameter of the proximal dome (*b*).

TABLE 1: Morphologic factors of aneurysms and occlusion rate

Morphologic Factors of Aneurysms Based on 3D Digital Subtraction Angiography	No. of Aneurysms in Each Occlusion Rate			Totals (n = 47)
	100% (n = 20)	≧95% (n = 11)	<95% (n = 16)	
Largest diameter				
Small (<5 mm)	13	4	7	25
Medium (≧5 mm)	7	7	9	22
Neck size				
Small (<4 mm)	17	10	12	39
Wide (≧4 mm)	3	1	4	8
Shape				
Simple	19	8	11	38
Complex	1	3	5	9
Dome-to-neck ratio				
<1.2	0	1	9	10
1.2–1.5	11	6	4	21
>1.5	9	4	3	16
Relationship to the major neighboring artery				
Separate	18	8	8	34
Involved	2	3	8	13

95% occlusion, loose packing, persistent opacification of the sac, or remnant neck.

Statistical Analysis.—Correlation of the occlusion rate with morphologic factors was analyzed statistically by the Mann-Whitney U test or Spearman's rank correlation test. The statistical level of significance was set at $P = .05$. Once significant morphologic factors were identified, stepwise regression analysis was performed to identify those factor(s) that significantly influenced the occlusion rate. For this analysis, nominal qualitative variables were transformed into quantitative variables (presence = 1, absence = 0).

Difficulty Score for Prediction of Endosaccular Packing with GDC.—When the factors that significantly influenced the occlusion rate were identified, a simple difficulty score based on these morphologic factors was calculated using the following grading system: 0, largest diameter less than 5 mm; 1, largest diameter greater than or equal to 5 mm; 0, dome-to-neck ratio greater than 1.5; 1, dome-to-neck ratio from 1.2 to 1.5; 2, dome-to-neck ratio less than 1.2; 0, neck size less than 4 mm; 1, neck size greater than or equal to 4 mm; 0, simple shape; 1, complex shape; 0, separate from neighboring artery; 1, involving neighboring artery. Thus, a high difficulty score determined by 3D-DSA findings should indicate the likelihood of failure of endosaccular packing with GDC. Finally, the difficulty score for each aneurysm was compared with results of endovascular treatment.

Results

Morphologic Features Determined by 3D-DSA Findings and Occlusion Rate

Of 47 aneurysms, 20 (43%) showed 100% occlusion, 11 (23%) showed greater than or equal to 95% occlusion, and 16 (34%) showed less than 95% occlusion immediately after embolization. The morphologic factors determined by 3D-DSA findings and the occlusion rates of the 47 aneurysms are summarized in Table 1. No significant correlation existed between occlusion rate and morphologic factors regarding largest diameter.

Neck Size.—One hundred percent occlusion was achieved in 17 (43.6%) of 39 aneurysms with small necks and in three (37.5%) of eight aneurysms with wide necks. Furthermore, greater than or equal to 95% occlusion was observed in 27 (69.2%) of 39 aneurysms with small necks and in four (50%) of eight aneurysms with wide necks.

Shape.—One hundred percent occlusion was achieved in 19 (50%) of 38 aneurysms with simple shapes and in one (11.1%) of nine aneurysms with

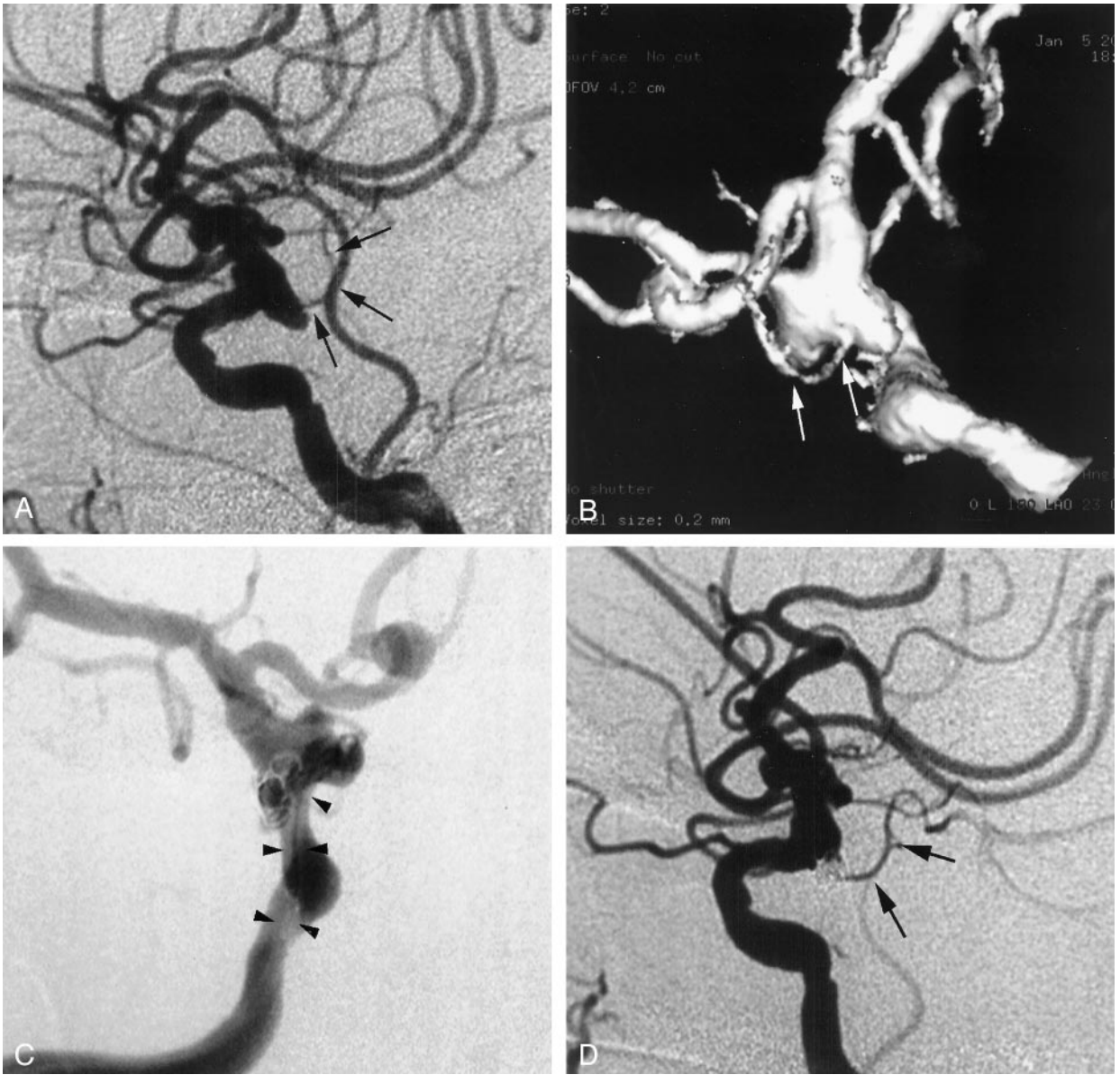

FIG 2. Ruptured internal carotid artery aneurysm.

A, Lateral 2D-DSA image. A wide-necked aneurysm can be seen at the origin of the posterior communicating artery (*arrows*). The relationship of the aneurysm to the posterior communicating artery is not clear in this image.

B, Surface shaded display image. Note the neck of the aneurysm and its involvement with the posterior communicating artery (*arrows*). The dome-to-neck ratio is 1.0 on this three-dimensional image. The calculated difficulty score is 3.

C, GDC procedure was performed with a double microcatheter (*arrowheads*) technique.

D, Lateral 2D-DSA image obtained immediately after GDC procedure shows incomplete occlusion (<95%) of the aneurysm and patent posterior communicating artery (*arrows*).

complex shapes. Furthermore, greater than or equal to 95% occlusion was observed in 27 (71.1%) of 38 aneurysms with simple shape and in four (44.4%) of nine aneurysms with complex shapes.

Dome-to-Neck Ratio.—One hundred percent occlusion was achieved in nine (56.3%) of 16 aneurysms with dome-to-neck ratios greater than 1.5, in 11 (52.4%) of 21 aneurysms with dome-to-neck ratios between 1.2 and 1.5, and in 0 (0%) of 10 aneurysms with dome-to-neck ratios less than 1.2. Furthermore, greater than or equal to 95% occlusion was observed in 13 (81.3%) of 16 aneurysms with dome-to-neck ratios greater than 1.5, in 17 (85%) of 20 aneurysms with dome-to-neck ratios between 1.2 and 1.5, and in one (10%) of 10 aneurysms with dome-to-neck ratios less than 1.2.

Relationship with Neighboring Artery.—One hundred percent occlusion was achieved in two (15.4%) of 13 aneurysms involving the neighboring artery and in 18 (52.9%) of 34 aneurysms without involvement of the neighboring artery (Figs 2 and 3). Steno-occlusive changes in the neighboring artery immediately after the procedure was observed in five (38%) of the 13 aneurysms involving the neighboring artery but was not observed in aneurysms without involvement of the neighboring artery.

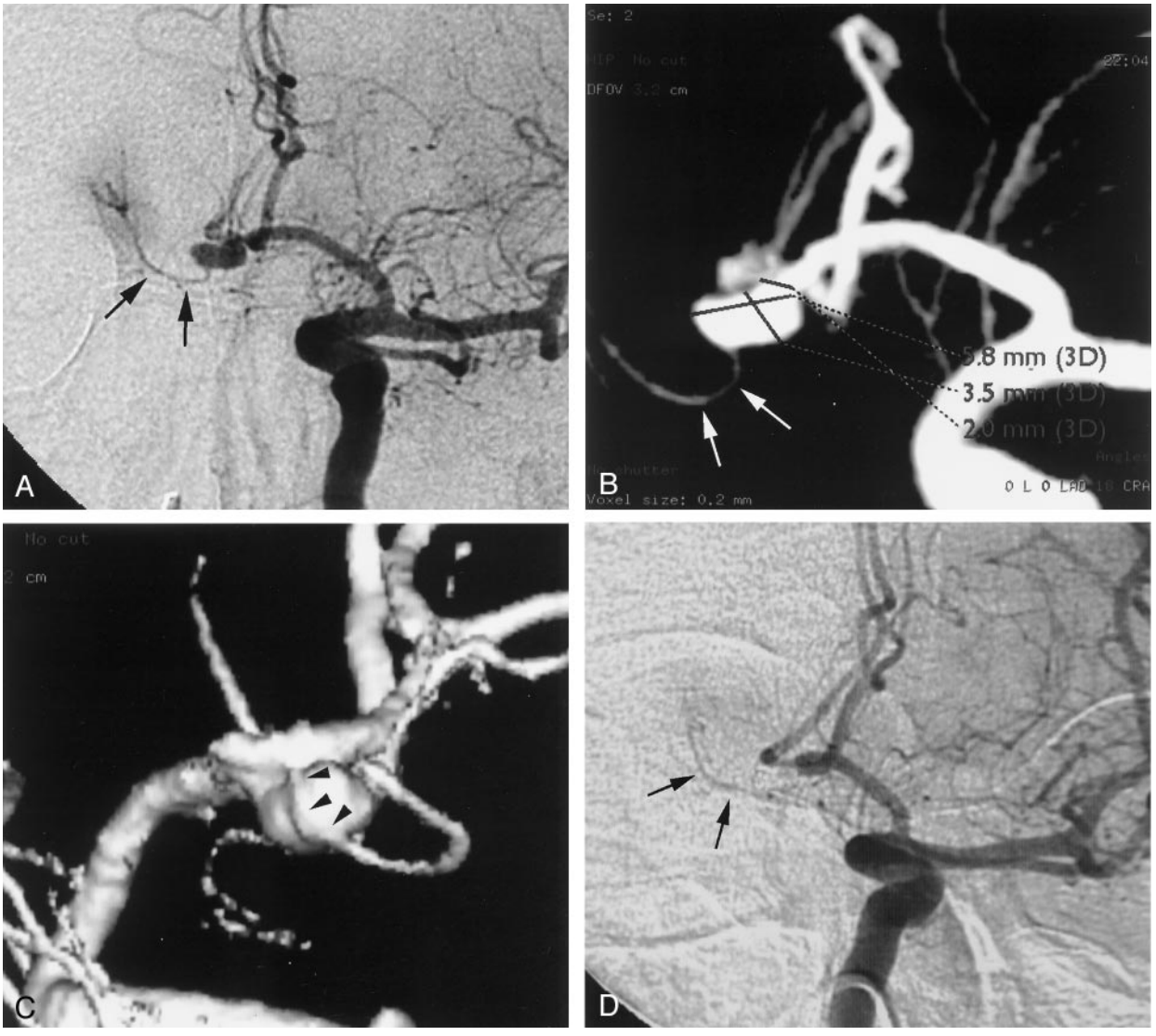

FIG 3. Ruptured aneurysm of the anterior communicating artery.

A, Right anterior oblique 2D-DSA shows aneurysm of the anterior communication artery with a dome-to-neck ratio of 1.8. A small perforating artery (*arrows*) is thought to originate from the aneurysmal dome.

B, MIP image of the 3D-DSA image shows aneurysm of the anterior communication artery with a dome-to-neck ratio of 1.8. A small perforating artery (*arrows*) is thought to originate from the aneurysmal dome.

C, Posterior surface shaded display image clearly shows that the perforating artery originates from the anterior cerebral artery (*arrowheads*), beyond the neck and running along the aneurysmal sac. Difficulty score is 0.

D, Right anterior oblique 2D-DSA image obtained immediately after the GDC procedure shows complete occlusion (100%) of the aneurysm with a patent perforating artery (*arrows*).

TABLE 2: Correlation matrix of coefficients

	Neck Size	Shape	Dome-to-Neck Ratio	Relationship to the Major Neighboring Artery
Neck size	1.0	−0.119	−2.58	0.257
Shape		1.0	0.286	0.257
Dome-to-neck ratio			1.0	−0.055
Relationship to the major neighboring artery				1.0

These four factors were found to correlate significantly with the occlusion rate: neck size ($P = .014$), shape ($P = .042$), dome-to-neck ratio ($P < .01$), and relationship with the neighboring artery ($P = .025$). The correlation coefficients are listed in Table 2. Using multivariate analysis, dome-to-neck ratio and relationship with the neighboring artery were found to be independent factors that significantly influenced the occlusion rate. The estimated regression coefficient (β) and the estimated standard error for these

TABLE 3: Difficulty score of aneurysms and occlusion rate

Difficulty Score	No. of Aneurysms in Each Occlusion Rate			Totals (n = 47)
	100% (n = 20)	≥95% (n = 11)	<95% (n = 16)	
0	9	4	1	14
1	10	4	2	16
2	1	3	9	13
3	0	0	4	4

two variables were 1.415 and 0.393, respectively, for dome-to-neck ratio and −7.13 and −0.366, respectively, for relationship with the neighboring artery.

Difficulty Score.—Difficulty score was calculated on the basis of dome-to-neck ratio and relationship to the neighboring artery by using the aforementioned simple grading system. Of 47 aneurysms, the difficulty score was 0 for 14 aneurysms, 1 for 16, 2 for 13, and 3 for four (Table 3). Of the 14 aneurysms with a difficulty score of 0, 13 (93%) showed greater than or equal to 95% occlusion (Fig 3) and one (7%) showed less than 95% occlusion. Furthermore, 14 (87.5%) of the 16 aneurysms with a difficulty score of 1 and four (30.2%) of the 13 aneurysms with a difficulty score of 2 showed at least greater than or equal to 95% occlusion. All four of the aneurysms with a difficulty score of 3 showed less than 95% occlusion. The difficulty score correlated significantly and negatively with the occlusion rate ($r = -0.64$, $P < .01$).

Complex techniques were used in 10 aneurysms. Of these, three had a difficulty score of 1, six had a difficulty score of 2, and one had a difficulty score of 3 (Fig 2).

Discussion

The occlusion rate of aneurysms by endosaccular packing with coils is influenced by a variety of factors related to the morphologic features of the aneurysm, including dome-to-neck ratio, size of the neck and dome, shape, and relationship to the major neighboring artery. However, these aneurysm-related features often cannot be characterized clearly on conventional biplane DSA images without multiple radiographic projections with various views. It is sometimes difficult to find a view that best defines these morphologic features on conventional DSA images with multiple projections. Recent technologic developments have allowed us to obtain three-dimensional reconstructed images by use of rotational angiography in a short time (≤8 minutes) (12). One can examine the image from any view with a high resolution and can measure the images at real time on the workstation. A precise calculation of the size of the aneurysm is often necessary for proper evaluation of the aneurysm. Tanoue et al (16) recently reported that the morphologic features of aneurysms determined by 3D-DSA findings correlate with those of direct examination during surgery and that the sizes of the aneurysms calculated with 3D-DSA images also correlate with those measured during surgery (16). These morphologic factors are accurately evaluated with 3D-DSA (11).

Dense packing of the coils within the aneurysmal sac can be achieved with less risk of migration of the coil into the parent artery when the treated aneurysm has a small dome size, a small neck, and a large dome-to-neck ratio, conditions that enhance the complete occlusion of the aneurysm (4, 13). A high success rate (80–85%) of complete occlusion can be achieved in such aneurysms (4, 6). In the present study, neck size and dome-to-neck ratio correlated with the occlusion rate, which is similar to the findings of previous studies (4, 6, 13). On the other hand, the success rate of complete occlusion of giant aneurysms by endosaccular embolization is very low. In our series, none of the aneurysms had a diameter greater than 12 mm. Therefore, the maximal diameter of these three parameters showed no significant correlation with the occlusion rate.

The occlusion rate is also influenced by other factors, including relationship with the neighboring artery, shape of the aneurysm, tortuousity of the access route, and experience of the operator. However, little attention has been paid to these factors in the past. The relationship of the aneurysm to the neighboring artery is important in determining the feasibility of the GDC procedure. Complete occlusion of an aneurysm involving a major artery is associated with a high risk of stenosis or occlusion of the main artery and can potentially result in ischemic changes after the procedure. Our study showed a significant correlation between this factor and the occlusion rate. Furthermore, steno-occlusive changes in the neighboring artery were observed in 38% of the aneurysms involving the neighboring artery. Thus, it is not only important to evaluate the neck size and dome-to-neck ratio but also the relationship of the aneurysm to the neighboring artery before embolization.

Dense packing of a sac and neck with complex shapes is often difficult and requires a higher degree of skill. Therefore, complete occlusion of aneurysms with complex shapes is more difficult than that of aneurysms with simple shapes. Tortuousity of the access route because of atherosclerotic changes would also impose technical difficulties. We interrupted the GDC procedure before the detachment of the first coil in three cases because of poor maneuverability of the microcatheter caused by significant tortuousity of the access route. However, the access route does not include only intracranial arteries but also extracranial arteries that could not be evaluated by 3D-DSA, and tortuousity of these arteries is difficult to evaluate objectively. Because the aim of our study was to determine the morphologic factors that

influence the success rate of complete occlusion of the aneurysms on the basis of 3D-DSA, this factor was excluded in this study.

In addition to aneurysm-related factors, the experience of the operator may also influence the outcome of the GDC procedure. Turjman et al (5) showed in their series that chronologic sequence correlated well with the success rate of aneurysmal occlusion. Before the current series, we performed endosaccular packing with coils in more than 15 cerebral aneurysms. We did not find differences in occlusion rate between the initial 23 procedures (100% in nine, ≥95% in seven, and <95% in seven) and the later 24 procedures (100% in 12, ≥95% in four, and <95% in nine) in this series, suggesting no learning curve, at least in our department.

The difficulty score devised in the present study and based on the findings of 3D-DSA can be easily calculated. Our results showed that the estimated score correlated with the difficulty of aneurysmal occlusion; 90% of aneurysms with a difficulty score of less than 2 showed greater than or equal to 95% occlusion. On the other hand, aneurysms with a difficulty score of less than or equal to 2 were difficult to occlude successfully by endosaccular packing and often required complex surgical techniques for completion of the GDC procedure. Although our difficulty score was designed to allow prediction of the results of endosaccular embolization of the cerebral aneurysms, it could also be applied for decision making regarding the treatment of cerebral aneurysms. However, selection of coil embolization for individual cases should be determined by assessment of both the difficulty score and surgical difficulty.

The proportion of aneurysms that were classified as having 100% occlusion in this series was lower than those reported previously by other groups (3, 4, 15, 17). Several reasons could explain the difference. First, our selection of coil embolization was restricted to poor surgical conditions. Only 34% of aneurysms had dome-to-neck ratios greater than 1.5 in our series. Debrun et al (4) reported difficulty in completely occluding aneurysms with low dome-to-neck ratios. In their study, complete occlusion was obtained in approximately half of 12 aneurysms with dome-to-neck ratios less than 2.0. Second, we used 3D-DSA for evaluation of the occlusion rate of the aneurysm. A small remnant neck could be shown using this technique, which cannot be identified by conventional 2D-DSA. In our study, analysis of the occlusion rate based on the use of 2D-DSA showed that five of 11 aneurysms with greater than or equal to 95% occlusion were evaluated as being 100% occluded. The degree of technical skill could also affect the occlusion rate. The use of the complex technique or the stent-assist technique should improve the occlusion rate, particularly in aneurysms with wide necks (4, 13, 18, 19). However, complete occlusion of the aneurysms with small dome-to-neck ratios involving neighboring arteries is often difficult and dangerous, even when these complex techniques are used.

Conclusion

This study has certain limitations, including the small number of patients studied and the retrospective nature of the study. Although a prospective study that includes a larger number of patients is necessary, our difficulty score based on 3D-DSA images is simple and provides clinically useful information for predicting aneurysmal occlusion by endosaccular embolization.

Acknowledgments

The authors thank Hideuki Murakami, MRT, Shinji Ando, MRT, and Kazutaka Nomura, MRT, for technical support in interventional-angiographic procedures.

References

1. Guglielmi G, Viñuela F, Dion J, Duckwiler G. **Electrothrombosis of saccular aneurysms via endovascular approach: part 2. preliminary clinical experience.** *J Neurosurg* 1991;75:8–14
2. Guglielmi G, Viñuela F, Sepetka I, Macellari V. **Electrothrombosis of saccular aneurysms via endovascular approach: part 1. electrochemical basis, technique, and experimental results.** *J Neurosurg* 1991;75:1–7
3. Viñuela F, Duckwiler G, Mawad M. **Guglielmi detachable coil embolization of acute intracranial aneurysm: perioperative anatomical and clinical outcome in 403 patients.** *J Neurosurg* 1997;86: 475–482
4. Debrun GM, Aletich VA, Kehrli P, Misra M, Ausman JI, Charbel F. **Selection of cerebral aneurysms for treatment using Guglielmi detachable coils: the preliminary University of Illinois at Chicago experience.** *Neurosurgery* 1998;43:1281–1297
5. Turjman F, Massoud TF, Sayre J, Viñuela F. **Predictors of aneurysmal occlusion in the period immediately after endovascular treatment with detachable coils: a multivariate analysis.** *AJNR Am J Neuroradiol* 1998;19:1645–1651
6. Fernandez Zubillaga A, Guglielmi G, Viñuela F, Duckwiler GR. **Endovascular occlusion of intracranial aneurysms with electrically detachable coils: correlation of aneurysm neck size and treatment results.** *AJNR Am J Neuroradiol* 1995;15:815–820
7. Bidaut LM, Laurent C, Piotin M, et al. **Second-generation three-dimensional reconstruction for rotational three-dimensional angiography.** *Acad Radiol* 1998;5:836–849
8. Heautot JF, Chabert E, Gandon Y, et al. **Analysis of cerebrovascular diseases by a new 3-dimensional computerized X-ray angiography system.** *Neuroradiology* 1998;40:203–209
9. Koppe R, Klotz E, Op de Beek J, Aerts H. **3D vessel reconstruction based on rotational angiography.** In: Lemke HU, ed. *Computer Assisted Radiology '95.* Berlin: Springer-Verlag; 1995:101–107
10. Missler U, Hundt C, Weismann M, Mayer T, Brückmann H. **Three-dimensional reconstructed rotational digital subtraction angiography in planning treatment of intracranial aneurysms.** *Eur Radiol* 2000;10:564–568
11. Anxionnat R, Bracard S, Ducrocq X, et al. **Intracranial aneurysms: clinical value of 3D digital subtraction angiography in the therapeutic decision and endovascular treatment.** *Radiology* 2001;218: 799– 808
12. Anxionnat R, Bracard S, Macho J, Da Costa E, Vaillant R, Launay L, Trousset Y, Romeas R, Picard L. **3D angiography: clinical interest: first applications in interventional neuroradiology.** *J Neuroradiol* 1998;25:251–262
13. Moret J, Cognard C, Weill A, Castaings L, Rey A. **The "remodeling technique" in the treatment of wide neck intracranial aneurysms: angiographic results and clinical follow-up in 56 cases.** *Intervent Neuroradiol* 1997;3:21–35
14. Baxter BW, Rosso D, Lownie SP. **Double microcatheter technique for detachable coil treatment of large, wide-necked intracranial aneurysms.** *AJNR Am J Neuroradiol* 1998;19:1176–1178
15. Cognard C, Weill A, Spelle L, et al. **Long-term angiographic follow-up of 169 intracranial berry aneurysms occluded with detachable coils.** *Radiology* 1999;212:348–356
16. Tanoue S, Kiyosue H, Kenai H, Nakamura T, Yamashita M, Mori H. **Three-dimensional reconstructed images after rotational an-**

giography in the evaluation of intracranial aneurysms: surgical correlations. *Neurosurgery* 2000;47:866–871
17. Byrne JV, Sohn MJ, Molyneux AJ, Chir B. **Five-year experience in using coil embolization for ruptured intracranial aneurysms: outcomes and incidence of late bleeding.** *J Neurosurg* 1999;90:656–663
18. Wilms G, Calenbergh FV, Stockx L, Demaerel P, Loon JV, Goffin J. **Endovascular treatment of a ruptured paraclinoid aneurysm of the carotid siphon activated using endovascular stent and endosaccular coil placement.** *AJNR Am J Neuroradiol* 2000;21:753–756
19. Phatouros CC, Sasaki TY, Higashida RT, et al. **Stent-supported coil embolization: the treatment of fusiform and wide-neck aneurysms and pseudoaneurysms.** *Neurosurgery* 2000;47:107–115